PROTEINS
STRUCTURE ■ FUNCTION ■ BIOINFORMATICS

# Isolation, kinetic analysis, and structural characterization of an antibody targeting the *Bacillus anthracis* major spore surface protein BclA

**Stewart D. Nuttall,[1]* Michelle L. Wilkins,[1] Victor A. Streltsov,[1] Luisa Pontes-Braz,[1] Olan Dolezal,[1] Hung Tran,[2] and Chun-Qiang Liu[2]***

[1] CSIRO Division of Materials Science and Engineering, 343 Royal Pde, Parkville, Victoria, 3052, Australia
[2] DSTO Human Protection and Performance Division, 506 Lorimer Street, Fishermans Bend, Melbourne, Victoria 3207, Australia

ABSTRACT

**One method of laboratory- or field-based testing for anthrax is detection of *Bacillus anthracis* spores by high-affinity, high specificity binding reagents. From a pool of monoclonal antibodies, we selected one such candidate (A4D11) with high affinity for tBclA, a truncated version of the *B. anthracis* exosporium protein BclA. Kinetic analysis utilising both standard and kinetic titration on a Biacore biosensor indicated antibody affinities in the 300 pM range for recombinant tBclA, and the A4D11 antibody was also re-formatted into scFv configuration with no loss of affinity. However, assays against *B. anthracis* and related *Bacilli* species showed limited binding of intact spores as well as significant cross-reactivity between species. These results were rationalized by determination of the three-dimensional crystallographic structure of the scFv-tBclA complex. A4D11 binds the side of the tBclA trimer, contacting a face of the antigen normally packed against adjacent trimers within the exosporium structure; this inter-spore interface is highly conserved between *Bacilli* species. Our results indicate the difficulty of generating a high-affinity antibody to differentiate between the highly conserved spore structures of closely related species, but suggest the possibility of future structure-based antibody design for this difficult target.**

Proteins 2011; 79:1306–1317.


**Key words: exosporium; biosensor; infectious disease; anthrax; scFv complex; merohedral twinning.**

## INTRODUCTION

*Bacillus anthracis* is a spore-forming, Gram-positive bacterium that is the etiological agent of anthrax. There are two major factors that determine the virulence of *B. anthracis* in its vegetative form, namely the poly γ-D-glutamic acid (PGA) capsule and the secreted tripartite protein toxin. The PGA capsule functions to protect the organism against phagocytosis and is poorly immunogenic.[1] The vegetative state propagates within the bloodstream of a mammalian host, secreting large quantities of toxins and resulting in massive edema, organ failure, and finally death of the host.[2] In their dormant state, *B. anthracis* spores are enclosed by a prominent loose fitting layer called the exosporium, which is composed of a basal layer within a nap of hair-like filaments formed by a single collagen-like protein, known as BclA.[3,4] This protein consists of a central collagen-like region (CLR), consisting of mostly GPT triplets,[3] and a C-terminal all-β structure with a jelly-fold topology.[5,6] The C-terminal globular domain is located on the exterior of the exosporium.[4] Formation of this core β structure is independent of the anchoring collagen-like region, and individual subunits are assembled into hexagonal plates consisting of three tightly associated subunits.[7]

BclA is synthesized only in sporulating cells; it is the most predominant protein with its C-terminal globular domain located on the exterior of the exosporium, and is directly exposed to the environment.[3] Thus, the protein not only represents a potential vaccine candidate to complement the protective immunity conferred by the current toxin-based vaccines,[8] but equally importantly represents an ideal target for antibody-based detection of *B. anthracis* spores.[7] Recently, several monoclonal antibodies specific to BclA have been produced from mice

Michelle L. Wilkins current address is CSIRO Livestock Industries, Australian Animal Health Laboratory, Victoria, 3220, Australia

Additional Supporting Information may be found in the online version of this article.

Grant sponsor: The Commonwealth of Australia (the Major National Research Facilities Program); Grant sponsor: The Australian Synchrotron Research Program

*Correspondence to: Stewart Nuttall, CSIRO Materials Science and Engineering, 343 Royal Pde, Parkville, Victoria, 3052, Australia; E-mail: Stewart.Nuttall@csiro.au (or) Chun-Qiang Liu, DSTO Human Protection and Performance Division, 506 Lorimer Street, Fishermans Bend, Melbourne, Victoria 3207, Australia. E-mail: chun.liu@dsto.defence.gov.au.

Received 30 August 2010; Accepted 10 November 2010
Published online 22 December 2010 in Wiley Online Library (wileyonlinelibrary.com).
DOI: 10.1002/prot.22971

immunized with purified *B. anthracis* spores and the exosporium.[9] Some of these antibodies have demonstrated the ability to distinguish spores of *B. anthracis* from closely related and more benign species, such as *Bacillus cereus* and *Bacillus thurigiensis*—a vital consideration for front-end reagents of diagnostic biosensors.[10] The use of recombinant BclA (or tBclA) is an attractive strategy for the production of antibodies with binding affinity for anthrax spores, considering that the majority of antibodies generated by whole-spore immunization target BclA, and with the added advantage that this approach obviates the need to cultivate, prepare and inactivate the spores or prepare the exosporium.

Here, we report the further production of five monoclonal antibodies from mice immunized directly with the truncated protein tBclA. We describe the detailed kinetics characterisation of one of these antibodies and its adaptation to recombinant single chain Fv (scFv) format.[11,12] We analyze the binding of antibody to bacterial spores, and correlate these results with an X-ray crystallographic structure of the tBclA-scFv complex.

## MATERIALS AND METHODS

### Bacterial strains, plasmids, and culture media

Strains of *Bacillus* species included gamma-inactivated spores from 14 wild type *B. anthracis* strains (designated BAC1002, BAC1008, BAC1055, BAC1056, BAC1124, BAC1125, BAC1126, BAC1128, BAC1131, BAC1153, BAC1207, BAC1224, BAC1225, and BAC1226, respectively) isolated from nine different countries, and seven strains belonging to *B. licheniformis* (BAC1021), *B. megaterium* (BAC1026), *B. mycoides* (BAC1027), *B. subtilis* (BAC1033), *B. thuringiensis* (BAC1036), *B. atrophaeus* (BAC1051), and *B. cereus* (BAC1232). The inactivated spores were kindly provided by the United States Critical Reagents Program, Joint Executive Office for Chemical and Biological Defense (http://www.jpeocbd.osd.mil/packs/Default.aspx?pg=1205). An attenuated *B. anthracis* strain (Sterne 34F2) from Colorado Serum Company was also used. Sterne 34F2 is devoid of the plasmid pXO2 but still contains pXO1, and the strain is $10^{-5}$–$10^{-7}$ fold less virulent than wildtype bacteria. *E. coli* TG1 was originally purchased from Stratagene (La Jolla, CA).

### Production and purification of monoclonal antibodies

Recombinant tBclA was produced in *E. coli* and purified as described previously.[7] The protein was emulsified with Freund's Complete Adjuvant and used to subcutaneously immunize female Balb/C mice (6–7 weeks) at 3-week intervals. Sera were taken after the third booster and screened by enzyme-linked immunosorbent assay (ELISA) for reactivity to the immunogen. Spleen cells were prepared from the animal with the highest titre and fused with NS/1 murine myeloma cell line. All screenings and selections were carried out by ELISA on culture fluid for reactivity to tBclA. Cells were cloned by limiting dilution and then expanded in serum free media. Monoclonal antibodies were harvested from the culture supernatants and purified using protein G affinity column. Purified antibodies were buffer exchanged in Phosphate Buffered Saline (PBS), pH 7.4, and stored at −80°C. ELISA was used to determine the isotypes of the murine mAbs by using isotype-specific reagents (Sigma-Aldrich, NSW, Australia).

### mRNA extraction, PCR, cloning, and sequencing

The A4D11 murine hybridoma cell line (IgG1/kappa isotype) was utilized for PCR amplification of variable heavy ($V_H$) and variable light ($V_L$) chain cDNA. Total RNA was extracted from $5 \times 10^6$ cells using TRIzol reagent (Invitrogen, VIC, Australia) and messenger RNA subsequently isolated using the Oligotex mRNA kit (Qiagen Pty Ltd, VIC, Australia). The $V_H$ and $V_L$ cDNAs were synthesized according to previously described methodology.[13] Resulting PCR products were ligated into pPCR-Script Amp SK (+) vector (Stratagene La Jolla, CA), sequenced, and analyzed for consensus $V_H$ and $V_L$ sequences.

For scFv construction the 35G-5 gene fragment was assembled by the Splice Overlap Extension (SOE) PCR method.[14] Specifically, $V_H$ and $V_L$ genes were first amplified using **S**A4D11$V_H$NcoI (GCCCAGCCGGCCATGGCTgaagt gaaactggtggagtctg) and **as**A4D11$V_H$ (accggaaccgccgccaccg gatccgccgccgcctgaggagacggtgaccgtggtccc) primers for $V_H$; and **s**A4D11$V_L$ (**TCCGGTGGCGGCGGTTCCGGT**GGTGGTGG GTCAcaaattgttctcacccagtctcc) and **as**A4D11$V_L$Not (gtggtgct cgagtgcggccgcccgtttgat**CtcGag**cttggtgcctccacc) primers for $V_L$. Resulting gene fragments (~350 bp) containing overlapping and complementary linker sequences at the 3′ end of $V_H$ and 5′ end of $V_L$ were assembled into an scFv fragment by SOE PCR, giving an ~700 bp scFv DNA fragment.

The 35G-5 scFv gene fragment was cloned into an "in-house" *E. coli* expression vector pGC[15] at *Sfi*I and *Not*I restriction sites. The pGC vector is a pUC19 derivative, incorporating an N-terminal cleavable pelB periplasmic targeting signal and C-terminal FLAG and His6 peptide epitopes for affinity purification. Ligations were transformed into *E. coli* TG1 cells, and putative positive colonies screened by DNA sequencing.

### Expression, purification, and analysis of recombinant proteins

Expression and purification of 35G-5 scFv was performed as previously described.[16,17] Following FLAG and Histrap affinity purification, protein peaks corresponding to scFv monomer, and dimer fractions were

further purified by size-exclusion chromatography on a Superdex 200 HR10/30 column (GE Healthcare, VIC, Australia) equilibrated in PBS.

### Surface plasmon resonance

IgG and scFv binding and kinetics were determined by measuring SPR in a Biacore T100 unit (GE Healthcare). For IgG analysis ~2000 response units (RU) of rabbit anti-mouse IgG (RAM Fc) were coupled to a Series S CM5 research grade chip using *N*-hydroxysuccinimide-*N*-ethyl-*N*dimethylamino-propyl-carboiimide chemistry as described by the manufacturer (GE Healthcare). Unless stated otherwise, all binding experiments were performed at 25°C in triplicate using HBS-EP+ (10 m*M* Hepes, 150 m*M* NaCl, 3 m*M* EDTA, 0.05% surfactant P20) as the running buffer.

### Kinetic analysis by surface plasmon resonance

Approximately 170 RU (response units; 1RU = 1 pg of protein/mm$^2$) of A4D11 IgG was captured for tBclA kinetic analysis with a contact time of 180 s and flow rate of 5 μL/min. Different concentrations of tBclA (10.8, 3.6, 1.2, 0.4, and 0 n*M*) were each injected over the captured IgG at a flow rate of 30 μL/min and contact time of 240 s and a dissociation time of 300 s. The sensor surface was regenerated between each binding reaction with glycine-HCL pH 1.5 with a flow rate of 30 μL/min and a contact time of 300 s. For each experiment, response data were processed using a reference surface, thereby allowing correction for bulk refractive index changes and any non-specific binding.[18] Data were double referenced using responses from blank injections.[19] To determine binding kinetics, data from each experiment were globally fitted to a 1:1 binding model that incorporated a mass transport component.[20]

### ScFv binding kinetics

ScFv classical and kinetic titration binding experiments were performed with tBclA immobilized on the chip surface (~50 RU). Freshly peak-purified monomeric 35G-5 scFv was serially diluted in running buffer (HBS-EP+) to working concentrations. For classical experiments, 35G-5 scFv at different concentrations (9, 3, 1, 0.333, 0.111, and 0 n*M*) were each injected over immobilized tBclA at a flow rate of 30 μL/min and contact time of 180 s and a dissociation time of 300 s. The tBclA surface was regenerated between each binding cycle with Gentle Elution Buffer (Pierce, Rockford) with a flow rate of 30 μL/min and a contact time of 20 s. Binding data were processed and fit to 1:1 binding model containing mass transport component as described above. For kinetic titration, within a single binding cycle, the 35G-5 scFv samples were injected sequentially at 90 μL/min in order of increasing concentration over both ligand and reference surfaces. The reference surface, an unmodified flow cell was used to correct for systematic noise and instrument drift.[20] Two buffer blanks binding cycles using the same injection regime as with 35G-5 scFv concentrations were injected prior and post to the scFv binding cycle. These "buffer-blank" responses were used for double referencing of the scFv binding data.[21] To determine binding kinetics, processed data from each binding experiment were fit to a kinetic titration model that was set up in BIAevaluation software (v 4.1) as described by Karlsson *et al.*[21]

### Crystallization and data collection

The complex of recombinant scFv (27,434 Da) and trimeric tBclA (3 × 16,738 Da) was collected as a single peak from gel filtration, concentrated to ~6 mg/mL in 20 m*M* Tris.HCl (pH 8.0), and set up as 400 nL hanging drops around 480 conditions at the Bio21 collaborative crystallization center (http://www.csiro.au/c3). Plates were incubated at 20°C. Final crystallization conditions were 0.2 *M* Na acetate, 20% PEG 3350, ~pH 7, and 0.2 *M* $MgCl_2$, 25% PEG 3350, 0.1 *M* Hepes pH 7.5. Diffraction data for a single crystal (in well solution plus 30% (v/v) glycerol as cryoprotectant) was collected with 180° rotation, 1° oscillation, and 5 s exposure at ~100 K using the Photon Factory BL17A beamline, Tsukuba, Japan. Initial data processing was conducted with HKL2000 package.[22] The crystal diffracted up to 3.1 Å resolution (Table I). Coordinates and structure factors have been deposited in the Protein Data Bank with accession number 3AB0.

### Structure determination and refinement

The data processing with HKL2000 gave similar statistics for the higher ($P4_132$, No 213) and lower ($P2_13$, No 198) cubic symmetry groups with cell parameter $a = b = c = 125.45$ Å. The molecular weight of the visible structure component of the complex is ~37,670 Da and the Matthews coefficient $V_m$ is 2.2 Å/Da for 1 or 2 tBclA-scFv complexes in the asymmetric unit for possible $P4_132$ or $P2_13$ space group symmetry, respectively. This is equivalent to a solvent of content of 43.6%. Twinning is possible with operator (*-h,k,l*) for the $P2_13$ symmetry and apparent symmetry for two fold perfect twin would be $P4_132$. However, twining was not suspected initially, and the structure was solved using molecular replacement technique in this space group using the program PHASER[23] within CCP4[24] using data reduced in the higher symmetry space group $P4_132$. The first search model was built using our previous tBclA crystal structure[7] (PDB 2Z5W). One independent molecule was identified in the asymmetric unit which

**Table I**
Diffraction Data and Refinement Statistics

| | tBclA-scFv |
|---|---|
| Beamline | PF BL17A |
| Wavelength (Å) | 1.0000 |
| Space Group | $P2_13$ |
| Twin operator and fraction ($\alpha$)[a] | (-*h*, *l*, *k*), 0.485 |
| Unit cell ($a = b = c$) (Å) | 125.45 |
| Resolution range (Å) | 44.4–3.1 (3.2–3.1)[b] |
| Used unique reflections | 11,525 |
| Test reflections[c] | 588 |
| Redundancy | 18.1 (5.4) |
| $R_{merged}$[d] | 0.17 (0.92) |
| $\chi^2_{merged}$[e] | 1.53 (1.01) |
| $<I/\sigma(I)>$ | 18.8 (1.0) |
| Data completeness (%) | 98.2 (80.0) |
| $R_{work}$[f] (%) | 19.9 (24.4) |
| $R_{free}$[f,c] (%) | 24.5 (38.6) |
| Rmsd bonds (Å), angles (°) | 0.006, 0.946 |
| No of atoms | 5316 |
| • (rms) chain A (Å$^2$) | 40.1 (1) |
| • (rms) chain B (Å$^2$) | 46.4 (1) |
| • (rms) chain C (Å$^2$) | 47.9 (1) |
| • (rms) chain D (Å$^2$) | 40.1 (1) |
| • (rms) chain E (Å$^2$) | 50.9 (1) |
| • (rms) chain F (Å$^2$) | 54.1 (1) |
| • (rms) chain W (Å$^2$) | 25.4 (1) |
| • (rms) overall (Å$^2$) | 46.2 (1) |
| $V_m$ and corresponding % solvent | 2.2, 43.6 |

[a]Refined in REFMAC.
[b]Values in parenthesis are for the highest shell.
[c]Represents ~5% of the data.
[d]$R_{merge} = \Sigma_{hkl}\Sigma_j|I_j - <I_j>|/\Sigma_{hkl}\Sigma_j|I_j|$.
[e]$\chi^2_{merge} = \Sigma_{hkl}\Sigma_j(I_j - <I_j>)^2/\Sigma_{hkl}\Sigma_j(\sigma_j^2 + <\sigma_j>^2)$, where *hkl* specifies unique indices, *j* indicates equivalent observations of *hkl*, $I_j$ and $\sigma_j^2$ are the observed intensities and their errors, and $<Ij>$ and $<\sigma_j>$ are the mean values.
[f]$R = \Sigma_{hkl}\ ||F_o| - |F_c||/\Sigma_{hkl}|F_o|$, where $|F_o|$ and $|F_c|$ are the observed and calculated structure factor amplitudes, respectively.

formed a trimer with 3-fold symmetry related molecules in the crystal lattice. The structure with tBclA molecule alone was refined to *R* values of 44%. At the next step the scFv molecule model was build using the single chain Fv antibody from PBD 1QOK.[25] Iterative crystallographic refinement and model building were conducted using REFMAC5[26] and XTALVIEW/MIFit,[27] respectively, and yielded a model for residues 80-215 for the tBclA chain, and 1–117 and 1–106 for the scFv heavy and light chains, respectively. The experimental data within $I/\sigma$ range from 2 to 1 up to the resolution of 3.1 Å were included in refinement, where over 50% data are still within 1 standard deviation of the mean. Following the convergence in standard REFMAC5 refinement, further improvement of *R* factors (over 2%) was achieved by refining all chains as separate rigid anisotropic domains with the TLS procedure (transition-libration-screw motion tensors refinement[28]). The libration tensor showed significant anisotropy. The final refinement of this model converged to $R = 0.22$ and high $R_{free} = 0.36$ indicating that the data required further analysis, in particular in respect of the twinning. It is known that the analysis of the moment of intensities can behave abnormally and more robust tests have to be utilized.[29] The Britton plot, H-test, and ML estimate performed by Xtriag program from the PHENIX system[30] (Supporting Information Figure 1) suggested near perfect merohedral (hemihedral) twinning with the average twin fraction estimate of 0.46. It showed that intensities related by the putative twin operator were highly correlated, resulting in an estimated twin fraction >0.4, even though the intensity statistics indicate that the structure is not twinned. Assuming that the measured crystal is a potential perfect twin, further refinements of the structure were conducted in the cubic $P2_13$ symmetry with twin fraction refined to 0.48 in REFMAC5. The TLS parameters for six separate chains of two tBclA-scFv complexes in asymmetric unit were also included in the refinement. The refinement statistic improved to $R = 19.9\%$ and $R_{free} = 24.5\%$ (Table I). Progress of the refinement was monitored using the $R_{free}$ statistic based on a test set encompassing 5% of the observed diffraction amplitudes. To reduce possible correlations introduced by the twinning, the test reflections were selected in thin resolution shells. The final model contained 718 residues and 14 water molecules with 98% of the residues with geometry in the favored and allowed regions of the Ramachandran plot (Supporting Information Figure 2). Supporting Information Figure 3 shows representative electron density in the area of contact between the tBclA and scFv molecules. The tBclA-scFv contact surface area was calculated with probe sphere radius 1.7 Å using the AREAIMOL program from the CCP4 suite.[24] The shape complementarity statistics was calculated with the SC[31] program of the CCP4 suite.

### Bioassay for bacterial spores

The binding assays for bacterial spores were carried out using ELISA, essentially as described previously.[7] Briefly, MaxiSorp 96 well plates (NUNC, Roskilde, Demnmark) were coated with gamma-irradiated spores (each at $5 \times 10^6$/mL) and blocked in skim milk. Primary antibodies used were scFv 35G-5 monomer (10 μg/mL) and scFv 35G-5 dimer (8 μg/mL), A4D11 (2 μg/mL), and S26 (2 μg/mL). The secondary antibody was a rabbit anti-mouse antibody conjugated to alkaline phosphatase from Sigma. Optical density was read at 405 nm with an ICN Titertek-Plus MS212 plate reader (Biomedicals, Meckenheim, Germany). Negative controls on the same plate contained no primary antibodies. Any signal that was at least twice the standard deviation after subtraction of its negative control signal was considered positive.

## RESULTS

### Isolation of anti-tBclA antibodies

Balb/C mice were immunized with truncated protein (tBclA) to raise monoclonal antibodies (MAbs) directed

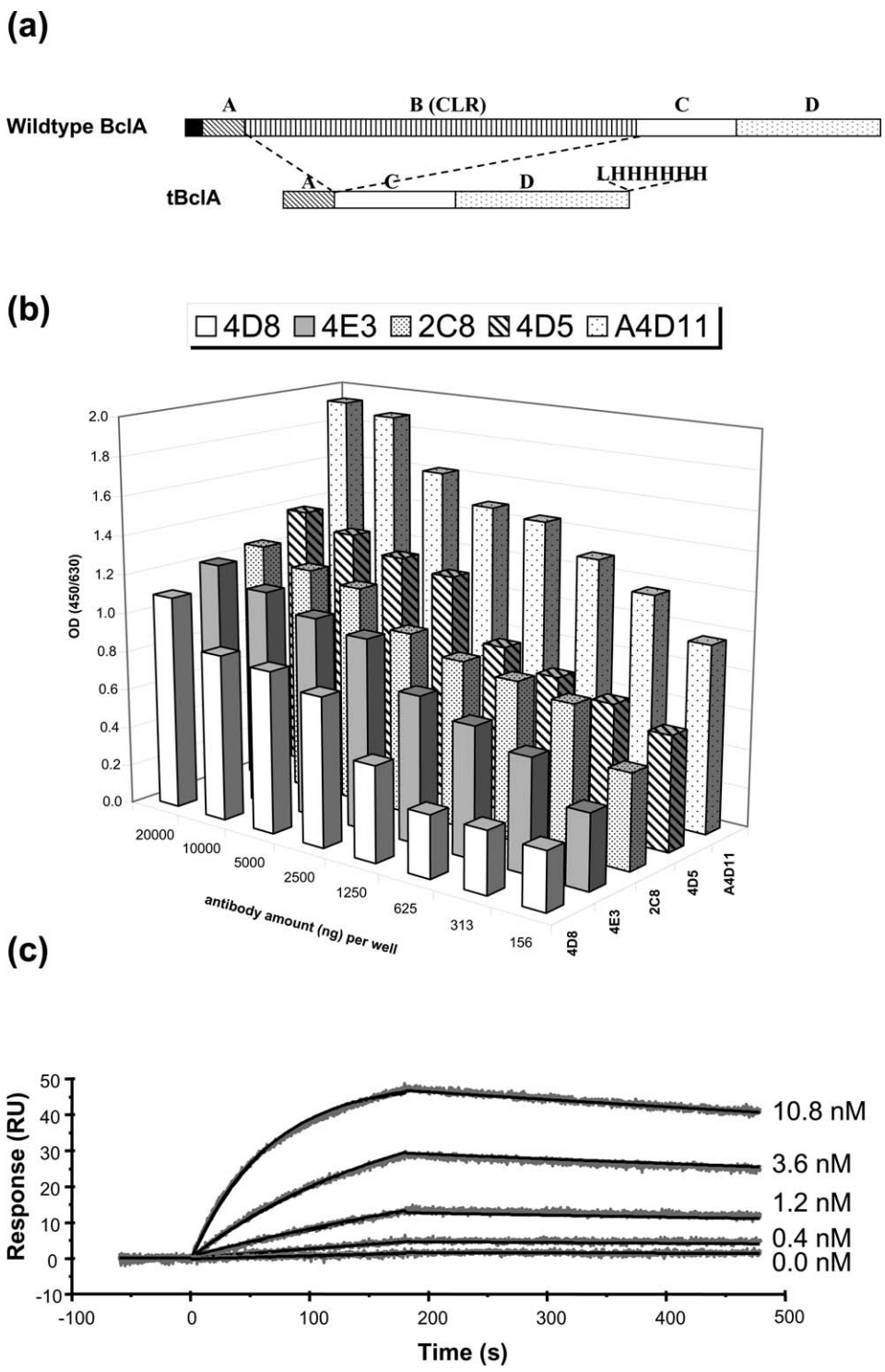


**Figure 1**

Monoclonal antibodies targeting tBclA. (**a**) Recombinant protein tBclA lacks the collagen-like region found in the native protein, and incorporates a Hexahistidine tag for affinity purification purposes. (**b**) Monoclonal antibodies 4D8, 4E3, 2C8, 4D5, and A4D11 bind immobilized tBclA by ELISA. (**c**) Biacore biosensor titration series for A4D11 monoclonal antibody (immobilized on the sensor surface) with increasing concentrations (0.4, 1.2, 3.6, and 10.8 n*M*) of tBclA protein as analyte.

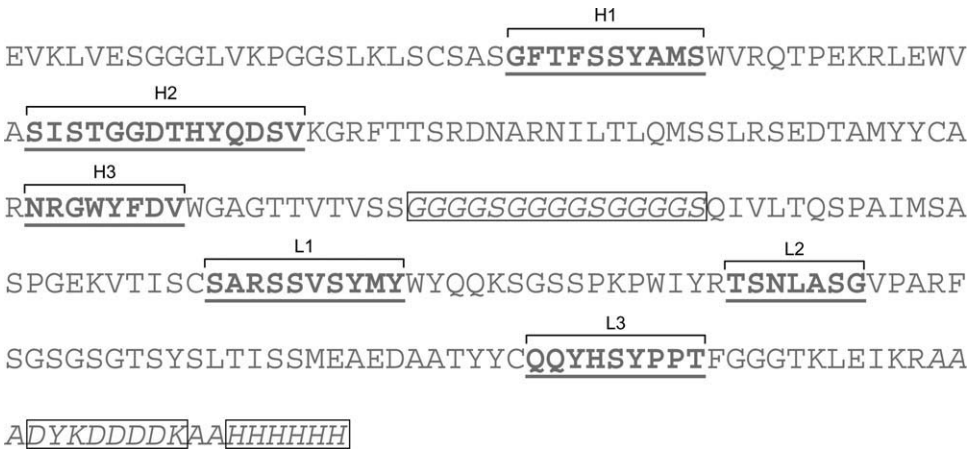


**Figure 2**

The A4D11 monoclonal antibody scFv fragment. Deduced amino acid sequence for anti-tBclA scFv 35G-5. Complementarity determining region (CDR) loops are indicated for the heavy (H1, H2, H3) and light (L1, L2, L3) antibody chains. The 15 residue VH-VL linker, and C-terminal FLAG and hexahistidine tag regions are boxed.

against the outer *B. anthracis* spore surface, rather than the connective collagen-like stalk regions [Fig. 1(a)]. Five MAbs were obtained; four (2C8, 4D5, 4D8, and 4E3) of the IgM class and one (A4D11) of the IgG class. These MAbs were purified and tested for their ability to bind immobilized tBclA by ELISA. Positive signals were detected for all five antibodies, with the signal from A4D11 being the most significant [Fig. 1(b)]. Initial spore-binding assays and biosensor data (results not shown) also suggested that A4D11 possessed superior spore-binding activity to the other antibodies. These results, combined with the relative advantages of working with an IgG isotype, led us to choose MAb A4D11 for further analysis.

In a series of kinetic experiments, affinity-purified A4D11 antibody was captured on a biosensor chip and the affinity determined for tBclA (as analyte) [Fig. 1(c)]. The kinetics fit a 1:1 binding model, with the final affinity determined at $\sim$ 330 pM (Table II, row 1). Interestingly, this strong interaction appeared to be mainly driven through the fast association rate constant ($k_a$ = 1.4 $\times$ $10^6$ $M^{-1}s^{-1}$), whilst the dissociation rate constant ($k_d$ = 4.5 $\times$ $10^{-4}$ $s^{-1}$) appeared to be on the lower side of average for the class of high affinity antibody–antigen interactions where the $K_D$ is less than 1 n*M* (OD, unpublished data).

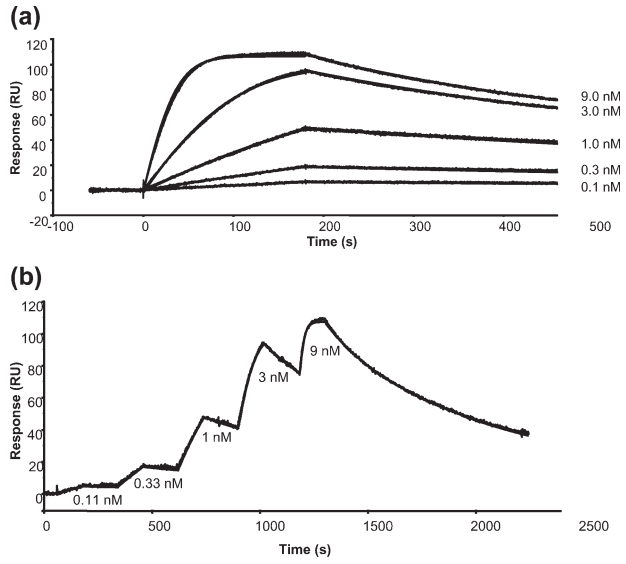


**Figure 3**

The A4D11 scFv antibody binds tBclA. **(a)** Triplicate data sets for the A4D11 (35G-5) scFv fragment (9, 3, 1, 0.33, and 0.11 n*M*) binding to immobilized tBclA. **(b)** Kinetic titration binding data set for the A4D11 (35G-5) scFv fragment (9, 3, 1, 0.33, and 0.11 n*M*) binding to immobilized tBclA.

## A4D11 scFv construction

To further explore the use of MAb A4D11 as a front end detection reagent for *B. anthracis* spores, we

**Table II**
Antibody Affinities

| Surface | Analyte | Method | $k_a$ ($M^{-1}s^{-1}$) | $k_d$ ($s^{-1}$) | $K_D$ (M) |
|---|---|---|---|---|---|
| A4D11 IgG | tBclA | Kinetics | 1.4 $\times$ $10^6$ | 4.5 $\times$ $10^{-4}$ | 3.3 $\times$ $10^{-10}$ |
| tBclA | 35G-5 scFv | Kinetic Titration | 6.8 $\times$ $10^6$ | 1.7 $\times$ $10^{-3}$ | 2.6 $\times$ $10^{-10}$ |
| tBclA | 35G-5 scFv | Kinetics | 7.5 $\times$ $10^6$ | 1.7 $\times$ $10^{-3}$ | 2.3 $\times$ $10^{-10}$ |

All measurements were performed at 25°C. Kinetic constants ($k_a$ and $k_d$) were determined from measurements using a Biacore T100 instrument. The equilibrium dissociation constant, $K_d$, is calculated from the ratio of the rate constants, $k_d/k_a$.

converted A4D11 to single chain Fv (scFv) format. This represents the minimal binding unit for $V_H$-$V_L$ antibodies and theoretically maximizes the binding activity:molecular weight ratio for coupling to a biosensor surface. Heavy and light chain coding sequences were amplified from cellular mRNA, cloned, and verified by comparison with N-terminal sequencing of affinity-purified antibody. The complete scFv was designated as clone 35G-5 and incorporates a $(Gly_4Ser)_3$ linker connecting the $V_H$ and $V_L$ domains, and sequential C-terminal FLAG and hexahistidine affinity tags (theoretical molecular weight 27,434 Da; Fig. 2). Database searches utilizing the sequenes of the complementarity determining regions (CDRs) revealed no close matches, suggesting that A4D11 is a novel antibody and certainly different from other Anthrax spore-targeting MAbs.

Recombinant protein 35G-5 was readily expressed into the *E. coli* periplasmic space and purified to homogeneity by sequential immobilized metal affinity chromatography ($Ni^{2+}$) and anti-FLAG affinity chromatography (data not shown). Gel filtration chromatrography revealed the presence of monomeric and dimeric species, typical of the results from scFv purifications,[32,33] which were individually collected. To determine whether 35G-5 scFv retained anti-tBclA binding, a series of biosensor experiments were again performed. In this instance, tBclA antigen was immobilized onto the sensor chip and freshly peak-purified monomeric 35G-5 scFv was used as analyte. Similar 1:1 affinity and kinetic profiles were obtained for 35G-5 compared to the parental monoclonal antibody [Fig. 3(a)]; the excellent 1:1 fit with no indication of biphasic binding (especially in the off-phase) further indicated that there was no scFv analyte heterogeneity. Again, the interaction was mainly driven through the fast association rate constant (Table II, row 3). We further confirmed the 35G-5 binding affinity utilizing the single-cycle kinetics approach, whereby increasing concentrations of monomeric 35G-5 scFv were sequentially injected over immobilized tBclA without regeneration of the chip between injections [Fig. 3(b)]. Again, the kinetic and affinity parameters correlated well with the results obtained from conventional kinetic measurements (Table II, row 2).

## Bioassay for *B. anthracis* spores

Next, we sought to validate A4D11 and the scFv 35G-5 (monomeric and dimeric forms) in biological assays utilising intact *B. anthracis* spores, in comparison to S26, a commercial anti-*B. anthracis* spore MAb. We tested the efficacy and specificity of these antibodies against a panel of gamma-inactivated spores from 14 different strains of *B. anthracis*, and seven strains of other *Bacilli* including the closely related species *B. mycoides*; *B. thuringiensis* and *B. cereus*. A4D11 was able to recognize, albeit with varying degrees of sensitivity, all *B. anthracis* strains tested, but failed to distinguish *B. anthracis* from, in particular, *B. mycoides*; *B. thuringiensis* and *B. cereus* [Fig. 4(a)]. In comparison, the commercial S26 MAb exhibited a higher specificity against related species, and generally higher reactivity, in this particular assay [Fig. 4(a)]. We also tested the 35G-5 monomeric and dimeric fractions against this spore panel [Fig. 4(b)]. In this assay, sensitivity was reduced compared to the parental antibody, a result we attribute to decreased detection by the anti-murine secondary antibody, while the dimeric fraction showed superior binding to the monomer fraction due to avidity affects. Notwithstanding, the overall pattern of reactivity was the same as for the parental A4D11 antibody, that is, no significant discrimination was observed between *B. anthracis* and related *Bacilli* species.

## Co-crystallization of A4D11 and tBclA

We next sought to rationalize the low levels of binding of A4D11 to *B. anthracis* spores, and the inability of MAb A4D11 to distinguish between closely related *Bacilli* species, by structural analysis. Affinity purified monomeric 35G-5 scFv and tBclA trimer were mixed in approximately stoichiometric quantities and separated by gel filtration. The molecular weight of the resulting complex was consistent with a trimeric protein species (~130 kDa) consisting of three tBclA molecules[7] and three scFv molecules (Fig. 5). The protein complex was isolated, concentrated to ~6 mg/mL, and placed into 480-condition crystallization trials. The rapid crystallization of native tBclA into hexagonal-shaped plates (Supporting Information Figure 4a) under a wide variety of conditions represented an impediment to these experiments. For example, under crystallization conditions of low pH (<pH 5.0) hexagonal crystals formed which lacked the scFv protein, indicative of dissociation of the complex and crystallization of tBclA alone. Few diffracting crystals formed under conditions of neutral pH, for example 0.2 *M* Na acetate, 20% PEG 3350, ~pH 7 (Supporting Information Figure 4b). However, determination of the structure for these crystals likewise revealed only tBclA molecules within the crystal lattice (results not shown).

In contrast, one set (only) of crystallization conditions (0.2 *M* $MgCl_2$, 25% PEG 3350, 0.1 *M* Hepes pH 7.5) reproducibly gave cuboidal-shaped crystals (Supporting Information Figure 4c), which contained the scFv−tBclA complex. The data to ~3.1 Å resolution were collected with apparent point group 432. However, the crystal was found to be merohedral twinning, with a twin ratio of 0.48 estimated by established methods (see Materials and Methods for details). The true space group was deduced to be $P2_13$ and the final structure was solved by molecular replacement to ~3.1 Å resolution (Table I), revealing three scFv molecules decorating the surface of the tBclA trimer [Fig. 6(a)]. This crystallographic structure sheds considerable light on the limited spore-binding capacity

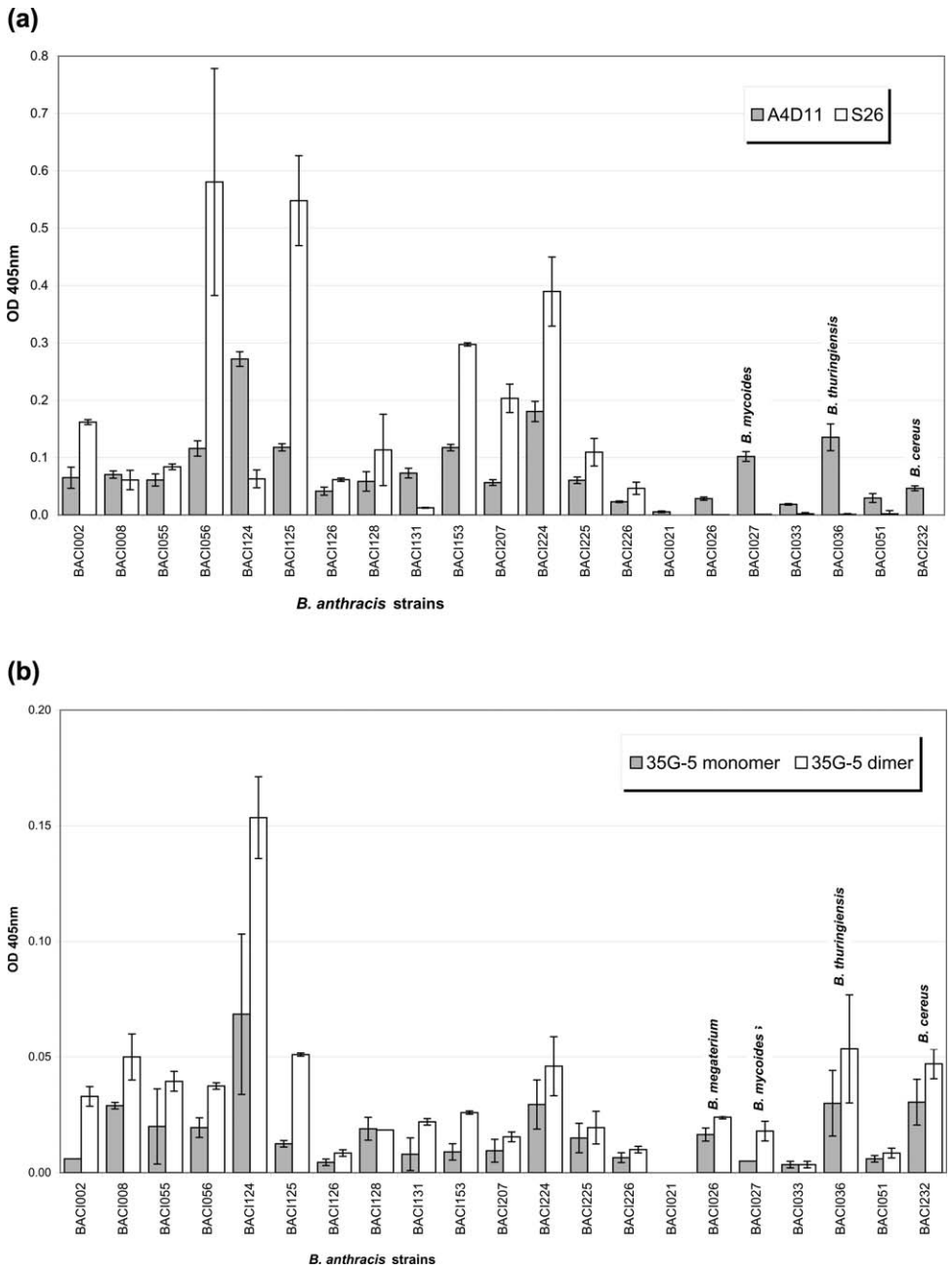


**Figure 4**

Detection of *Bacilli* spores by A4D11 monoclonal antibody and scFv. (**a**) Binding of A4D11 monoclonal antibody and S26 (a commercial MAb from HyTest Ltd), to gamma-irradiated *Bacillus* spores (each at $5 \times 10^5$ spores/mL). The assay was performed in duplicate and signals were plotted as average optical readings of the replicate. (**b**) Spore assay as for (a) except recombinant 35G-5 scFv monomeric and dimeric fractions derived from monoclonal antibody A4D11.

of MAb A4D11, as rather than contacting the environmentally exposed extracellular face of the tBclA trimer, the antibody binds to the side of tBclA trimer [Fig. 6(b)]. This surface is predicted to be accessible for *in vitro* assays utilising recombinant protein, such as ELISA and biosensor, but occluded in the native exosporium due to the close packing between adjacent trimeric subunits, mediated by the collagen-like stalk of the intact BclA which anchors the molecule to the spore surface.[4,36]

A4D11 binding contact is mediated principally through the antibody CDR regions with a contact area (probe radius 1.7 Å) of ~872 Å$^2$ [Fig. 6(c)], with the majority of contacts from the variable light chain domain loop regions (Table III). Similarly, the residues contacted

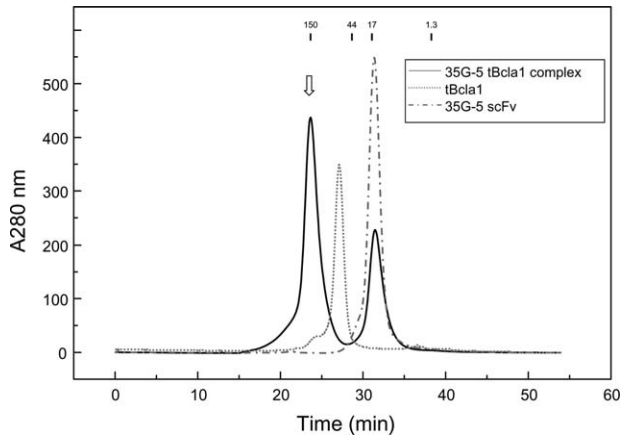


**Figure 5**

Isolation of the tBclA – A4D11 scFv complex. Excess gel filtration-purified A4D11 35G-5 scFv monomer (dashed line) was added to tBclA trimer (dotted line) and analyzed on a Superdex 200 HR 10/30 column. The resultant complex (solid line; arrowed) was collected and concentrated for crystallization trials.

by the A4D11 antibody are highly conserved between different *Bacilli* species (Supporting Information Figure 5), providing a rationale for the lack of inter-species discrimination. The shape complementarity between the two proteins (Sc)[31] of 0.58(9) (average for all chains; probe radius 1.7 Å,) is within the standard deviation of the common value for antibody-protein antigen interfaces.

## DISCUSSION

BclA is the predominant and surface-exposed protein that constitutes the *B. anthracis* exosporium[3,4,37] and it represents an attractive target for detection of spores indicative of anthrax. Current detection reagents either under development or commercially available include (predominantly) murine monoclonal antibodies[9]; bacteriophage-selected antibody fragments,[38] and novel binding reagents based on non-immunoglobulin scaffolds such as the Leucine Rich Repeat proteins from Lampreys.[39] Most of the antibodies raised against the exosporium are also highly reactive with BclA.[9,38,39] The majority of the current antibodies still suffer from cross-reactivity with closely related *Bacilli* species, such as *B. cereus* and *B. thuringiensis.*[9]

We sought to further fine-tune the murine anti-spore response by immunizing mice with just the surface-exposed C-terminal domain of BclA (tBclA), and were successful in obtaining the A4D11 antibody. The affinity of this antibody, in the picomolar range, is well within the biologically useful range and of sufficient affinity for use in an *in vitro* detection system. Slight differences in measured association and dissociation rate constants ($k_a$ and $k_d$) for the mature antibody compared to the scFv may be explicable by the differences in experimental set up and by the rapid association of antibody with antigen. Potential mass transfer limited condition effects may have influenced both the association and dissociation binding phases resulting in measured differences in $k_a$ and $k_d$. The correlation of the kinetic titration and conventional biosensor techniques both give us confidence in our affinity measurement, and highlight the potential usefulness of kinetic titration for analysis of antibody fragments especially in cases where rapid turnover of a large number of antibody-antigen interactions is required or when protein surface regeneration has proven to be difficult.

In our hands, spore-binding assays with A4D11, both in natural and scFv forms, revealed both poor activity and inter-species cross reactivity. The determination of a three dimensional structure nicely rationalized the apparent contradiction between high *in vitro* and this low *in vivo* activity. The A4D11 antibody targets the face of tBclA exposed at the side of the trimer and expected to be packed against adjacent trimers in the spore lattice,[4,40] an interaction mediated by the extended collagen-like stalk regions present in the intact BclA molecule (but absent in our truncated tBclA form). However, recognition of an epitope not readily accessible in intact spores is not necessarily fatal to development of a diagnostic assay. For example, the commercial MAb SA26, which recognised *B. anthracis* when tested on gamma-inactivated spores, may not be as efficient at recognising freshly prepared spores (data not shown). Thus, the target antigen may only be accessible to antibodies through the damaged spore surface following prolonged storage or gamma irradiation.[41] Additionally, for field operations, where both speed and accuracy are of paramount importance in protecting individuals against bioterrorist attacks, all samples that are identified positive by an immunoassay will be subjected to at least a second independent confirmative assay, such as PCR, which can serve to distinguish different *Bacilli* species. Similarly, humanised forms of A4D11 antibodies may have potential as immunopassive therapy agents against anthrax, as administration of rabbit anti-BclA antibodies significantly delayed the death of mice against spore lethal challenge and also decreased intramacrophage spore germination.[8] It should be noted that the specificity of an antibody is often of lesser concern in therapeutics than in detection, and it is in this context that a humanised A4D11 may find its greatest utility.

Our results illustrate the difficulties in obtaining a suitable antibody with both high specificity and exquisite sensitivity against highly conserved targets such as *Bacilli* spores. It may well be that the external surface of the spore coat, evolved to a high degree of surface resilience, also contributes to the character of low immunogenicity and surface complementarity. The trimer outer-facing

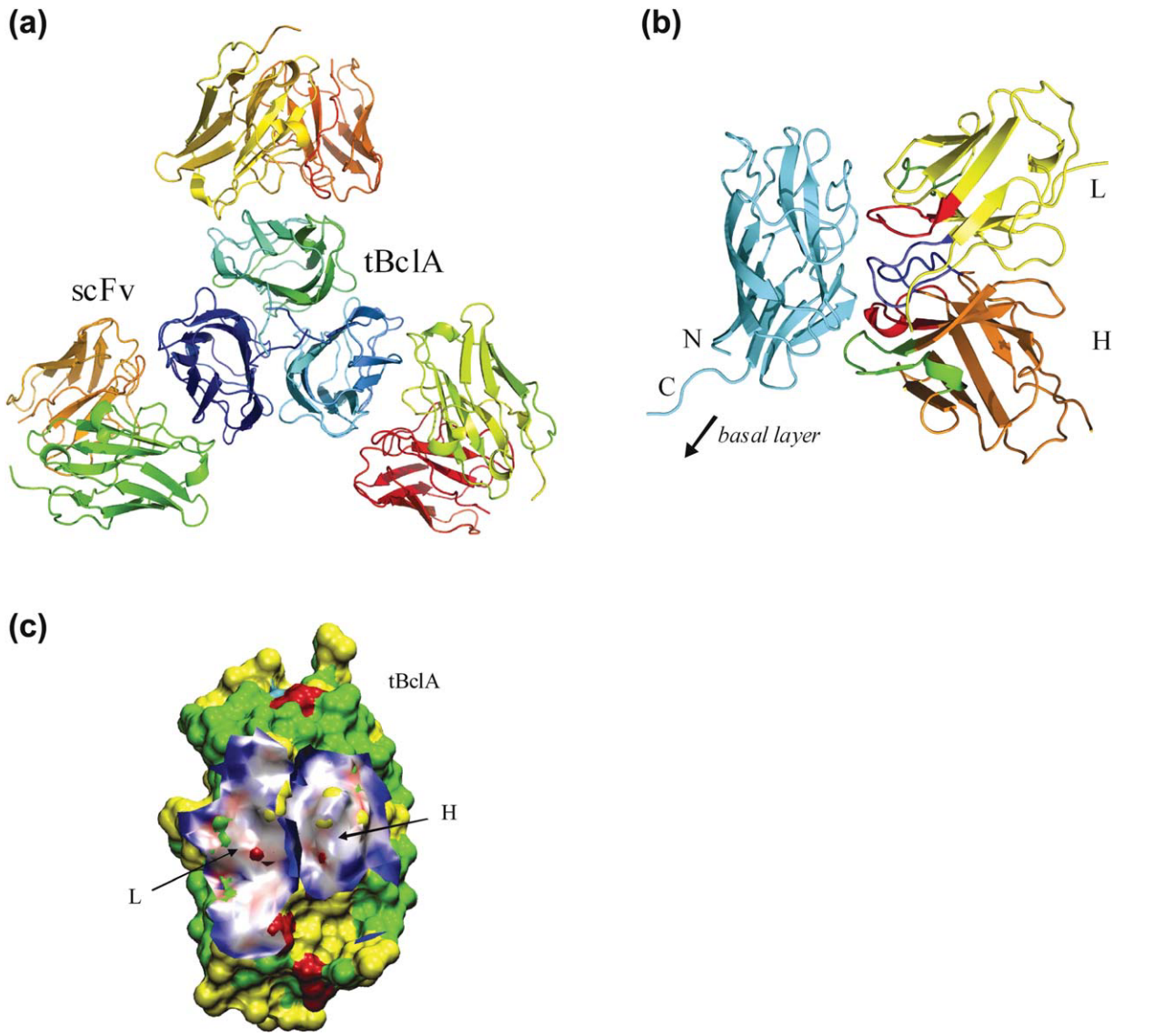


**Figure 6**

Structure of the tBclA-A4D11 scFv complex. (**a**) Cartoon representation of the scFv-tBclA structure as a trimer viewed along the 3-fold axis. (**b**) Side view of the tBclA monomer (left) with the scFv (right) light (L) and heavy (H) chains interacting through L1/H1 (red), L2/H2 (green), and L3/H3 (blue) complementarity determining regions. In the native BclA molecule, the globular tBclA domain is oriented toward and attached to the spore basal layer through a collagen-like region. (**c**) Surface representation of the tBclA molecule coloured by residue type (acidic–red, basic–cyan, polar–green, and nonpolar–yellow) with the "footprint" (distance threshold of 8 Å) of the interface between tBclA and A4D11 scFv proteins coloured by shape complementarity (from pink to blue). The picture was generated by using VMD[34] with Intersurf plugin.[35]

(apical) surface is formed by multiple loops (four loops from each monomer) and this flexibility (dynamics) is reflected in the higher values of atomic displacement parameters in the structural refinement. In addition, these mainly hydrophobic loops readily participated in interactions with the opposite surface of an adjacent trimer, producing a hexamer in the tBclA crystal structure.[7] Both the flexibility and accessibility of the apical trimer surfaces may thus have adversely affected development of suitable antibodies. Not-with-standing, the existence of a crystallographic structure for A4D11 in complex with tBclA raises the possibility of future application of structure-guided protein engineering to improve the affinity and specificity of this antibody, especially toward improving the shape complementarity and the targeting of residues of tBclA not conserved between *Bacilli* strains. This may be by incorporation of conventional point mutations, or by more sophisticated CDR loop extension, in particular targeting the variable heavy domain loops which are here underrepresented in crystal contacts. Such antibodies and their derivatives may serve as high specificity and high affinity detection reagents for incorpora-

**Table III**
tBclA–scFv Contacts <4 Å

| tBclA–scFv | Distance (Å) | CDR |
|---|---|---|
| Ser119 OG–Asp56 OD1 | 3.84 | H2 |
| Ser119 OG–Asp56 OD2 | 2.73 | H2 |
| Gln120 O–Asp56 OD2 | 3.25 | H2 |
| Gln120 O–Ser52 OG | 3.47 | H2 |
| Leu121 O–Thr53 N | 3.15 | H2 |
| Leu121 O–Thr53 OG1 | 3.50 | H2 |
| Asp122 OD2–Gly100 N | 2.81 | H3 |
| Asp122 OD2–Gly100 O | 3.74 | H3 |
| Ile101 O–Asn53 ND2 | 3.61 | L2 |
| Asn102 OD1–Tyr32 OH | 3.29 | L1 |
| Asn102 O–Arg50 NE | 3.79 | L2 |
| Asp103 OD1–Tyr49 OH | 3.79 | L2 |
| Gln154 OE1–Tyr32 OH | 2.68 | L1 |
| Gln154 NE2–Tyr32 OH | 3.00 | L1 |
| Asn156 OD1–His92 O | 3.18 | L3 |
| Asn156 O–His92 O | 3.27 | L3 |
| Asn156 O–Ser31 OG | 2.77 | L1 |
| Gly157 O–Ser31 OG | 3.46 | L1 |
| Glu190 OE1–His92 NE2 | 2.79 | L3 |
| Glu190 OE1–Tyr91 OH | 3.88 | L3 |
| Glu190 OE2–Tyr91 OH | 3.83 | L3 |

tion as the future front ends of biosensors for the detection of *B. anthracis*-based biological warfare agents.

## ACKNOWLEDGMENTS

We thank Ms Anna Raicevic for assistance with cloning, Mr Nick Bartone for N-terminal sequencing, Dr Janet Newman for advice on crystallography, and Drs Greg Coia and Remy Robert for critical reading of the manuscript. We thank The Photon Factory Synchrotron (Japan) for access to beamline 17A which was supported by the Australian Synchrotron Research Program, which is funded by the Commonwealth of Australia under the Major National Research Facilities Program.

## REFERENCES

1. Wang TT, Lucas AH. The capsule of Bacillus anthracis behaves as a thymus-independent type 2 antigen. Infect Immun 2004;72:5460–5463.
2. Dixon TC, Meselson M, Guillemin J, Hanna PC. Anthrax. N Engl J Med 1999;341:815–826.
3. Sylvestre P, Couture-Tosi E, Mock M. A collagen-like surface glycoprotein is a structural component of the Bacillus anthracis exosporium. Mol Microbiol 2002;45:169–178.
4. Boydston JA, Chen P, Steichen CT, Turnbough CL, Jr. Orientation within the exosporium and structural stability of the collagen-like glycoprotein BclA of Bacillus anthracis. J Bacteriol 2005;187:5310–5317.
5. Salamitou S, Rety S, Le Hegarat F, Leblon G, Lewit-Bentley A. The use of high halide-ion concentrations and automated phasing procedures for the structural analysis of BclA, the major component of the exosporium of Bacillus anthracis spores. Acta Crystallographica 2005;61(Pt 3):344–349.
6. Rety S, Salamitou S, Garcia-Verdugo I, Hulmes DJ, Le Hegarat F, Chaby R, Lewit-Bentley A. The crystal structure of the Bacillus anthracis spore surface protein BclA shows remarkable similarity to mammalian proteins. J Biol Chem 2005;280:43073–43078.
7. Liu CQ, Nuttall SD, Tran H, Wilkins M, Streltsov VA, Alderton MR. Construction, crystal structure and application of a recombinant protein that lacks the collagen-like region of BclA from Bacillus anthracis spores. Biotechnol Bioeng 2008;99:774–782.
8. Brahmbhatt TN, Darnell SC, Carvalho HM, Sanz P, Kang TJ, Bull RL, Rasmussen SB, Cross AS, O'Brien AD. Recombinant exosporium protein BclA of Bacillus anthracis is effective as a booster for mice primed with suboptimal amounts of protective antigen. Infect Immun 2007;75:5240–5247.
9. Swiecki MK, Lisanby MW, Shu F, Turnbough CL, Jr., Kearney JF. Monoclonal antibodies for Bacillus anthracis spore detection and functional analyses of spore germination and outgrowth. J Immunol 2006;176:6076–6084.
10. Pejcic B, De Marco R, Parkinson G. The role of biosensors in the detection of emerging infectious diseases. Analyst 2006;131:1079–1090.
11. Honegger A. Engineering antibodies for stability and efficient folding. Handb Exp Pharmacol 2008;181:47–68.
12. Weisser NE, Hall JC. Applications of single-chain variable fragment antibodies in therapeutics and diagnostics. Biotechnol Adv 2009;27:502–520.
13. Gilliland LK, Norris NA, Marquardt H, Tsu TT, Hayden MS, Neubauer MG, Yelton DE, Mittler RS, Ledbetter JA. Rapid and reliable cloning of antibody variable regions and generation of recombinant single chain antibody fragments. Tissue Antigens 1996;47:1–20.
14. Horton RM, Hunt HD, Ho SN, Pullen JK, Pease LR. Engineering hybrid genes without the use of restriction enzymes: gene splicing by overlap extension. Gene 1989;77:61–68.
15. Coia G, Ayres A, Lilley GG, Hudson PJ, Irving RA. Use of mutator cells as a means for increasing production levels of a recombinant antibody directed against Hepatitis B. Gene 1997;201:203–209.
16. Dolezal O, Pearce LA, Lawrence LJ, McCoy AJ, Hudson PJ, Kortt AA. ScFv multimers of the anti-neuraminidase antibody NC10: shortening of the linker in single-chain Fv fragment assembled in V(L) to V(H) orientation drives the formation of dimers, trimers, tetramers and higher molecular mass multimers. Protein Eng 2000;13:565–574.
17. Nuttall SD, Krishnan UV, Hattarki M, De Gori R, Irving RA, Hudson PJ. Isolation of the new antigen receptor from wobbegong sharks, and use as a scaffold for the display of protein loop libraries. Mol Immunol 2001;38:313–326.
18. Papalia GA, Baer M, Luehrsen K, Nordin H, Flynn P, Myszka DG. High-resolution characterization of antibody fragment/antigen interactions using Biacore T100. Anal Biochem 2006;359:112–119.
19. Myszka DG. Improving biosensor analysis. J Mol Recognit 1999;12:279–284.
20. Myszka DG, He X, Dembo M, Morton TA, Goldstein B. Extending the range of rate constants available from BIACORE: interpreting mass transport-influenced binding data. Biophys J 1998;75:583–594.
21. Karlsson R, Katsamba PS, Nordin H, Pol E, Myszka DG. Analyzing a kinetic titration series using affinity biosensors. Anal Biochem 2006;349:136–147.
22. Otwinowski Z, Minor W. Processing of X-ray diffraction data collected in oscillation mode. 1997;276:307–326.
23. Vagin A, Teplyakov A. MOLREP: An Automated Program for Molecular Replacement. J Appl Crystallogr 1997;30:1022–1025.
24. CCP4. The CCP4 suite: programs for protein crystallography. Acta Crystallographica 1994;50(Pt 5):760–763.
25. Boehm MK, Corper AL, Wan T, Sohi MK, Sutton BJ, Thornton JD, Keep PA, Chester KA, Begent RH, Perkins SJ. Crystal structure of the anti-(carcinoembryonic antigen) single-chain Fv antibody MFE-23 and a model for antigen binding based on intermolecular contacts. Biochem J 2000;346(Pt 2):519–528.
26. Murshudov GN, Vagin AA, Dodson EJ. Refinement of macromolecular structures by the maximum-likelihood method. Acta Crystallographica 1997;53(Pt 3):240–255.
27. McRee DE. XtalView/Xfit--A versatile program for manipulating atomic coordinates and electron density. J Struct Biol 1999;125:156–165.

28. Winn MD, Isupov MN, Murshudov GN. Use of TLS parameters to model anisotropic displacements in macromolecular refinement. Acta Crystallographica 2001;57(Pt 1):122–133.
29. Padilla JE, Yeates TO. A statistic for local intensity differences: robustness to anisotropy and pseudo-centering and utility for detecting twinning. Acta Crystallographica 2003;59(Pt 7):1124–1130.
30. Adams PD, Afonine PV, Bunkoczi G, Chen VB, Davis IW, Echols N, Headd JJ, Hung LW, Kapral GJ, Grosse-Kunstleve RW, McCoy AJ, Moriarty NW, Oeffner R, Read RJ, Richardson DC, Richardson JS, Terwilliger TC, Zwart PH. PHENIX: a comprehensive Python-based system for macromolecular structure solution. Acta Crystallographica 2010;66 (Pt 2):213–221.
31. Lawrence MC, Colman PM. Shape complementarity at protein/protein interfaces. J Mol Biol 1993;234:946–950.
32. Kortt AA, Dolezal O, Power BE, Hudson PJ. Dimeric and trimeric antibodies: high avidity scFvs for cancer targeting. Biomol Eng 2001;18:95–108.
33. Dolezal O, De Gori R, Walter M, Doughty L, Hattarki M, Hudson PJ, Kortt AA. Single-chain Fv multimers of the anti-neuraminidase antibody NC10: the residue at position 15 in the V(L) domain of the scFv-0 (V(L)-V(H)) molecule is primarily responsible for formation of a tetramer-trimer equilibrium. Protein Eng 2003;16:47–56.
34. Humphrey W, Dalke A, Schulten K. VMD: visual molecular dynamics. J Mol Graph 1996;14:33–38,27–38.
35. Ray N, Cavin X, Paul JC, Maigret B. Intersurf: dynamic interface between proteins. J Mol Graph Model 2005;23:347–354.
36. Sylvestre P, Couture-Tosi E, Mock M. Contribution of ExsFA and ExsFB proteins to the localization of BclA on the spore surface and to the stability of the bacillus anthracis exosporium. J Bacteriol 2005;187:5122–5128.
37. Steichen C, Chen P, Kearney JF, Turnbough CL, Jr. Identification of the immunodominant protein and other proteins of the Bacillus anthracis exosporium. J Bacteriol 2003;185:1903–1910.
38. Mechaly A, Zahavy E, Fisher M. Development and implementation of a single-chain Fv antibody for specific detection of Bacillus anthracis spores. Appl Environ Microbiol 2008;74:818–822.
39. Herrin BR, Alder MN, Roux KH, Sina C, Ehrhardt GR, Boydston JA, Turnbough CL, Jr., Cooper MD. Structure and specificity of lamprey monoclonal antibodies. Proc Natl Acad Sci U S A 2008;105:2040–2045.
40. Ball DA, Taylor R, Todd SJ, Redmond C, Couture-Tosi E, Sylvestre P, Moir A, Bullough PA. Structure of the exosporium and sublayers of spores of the Bacillus cereus family revealed by electron crystallography. Mol Microbiol 2008;68:947–958.
41. Williams DD, Turnbough CL, Jr. Surface layer protein EA1 is not a component of Bacillus anthracis spores but is a persistent contaminant in spore preparations. J Bacteriol 2004;186:566–569.